Impurity-induced modulations of orders in *d*-wave superconductors

Guo-Qiao Zha,[1,2,*] Yan Chen,[3] F. M. Peeters,[2] and Shi-Ping Zhou[1]
[1]*Department of Physics, Shanghai University, Shanghai 200444, China*
[2]*Departement Fysica, Universiteit Antwerpen, Groenenborgerlaan 171, B-2020 Antwerpen, Belgium*
[3]*Laboratory of Advanced Materials and Department of Physics, Fudan University, Shanghai 200433, China*
(Received 20 March 2009; revised manuscript received 12 July 2009; published 31 August 2009)

By using a model Hamiltonian with competing antiferromagnetic (AFM) and *d*-wave superconductivity orders, the impurity-induced structures of orders in *d*-wave superconductors is investigated. We find that the transition between one-dimensional stripe and two-dimensional checkerboardlike modulation around a single nonmagnetic impurity can take place as the strength of the AFM interaction U or the impurity scattering strength V_0 is varied. It is also found that the impurity-induced stripe can first transit to checkerboardlike modulation and then disappears with increasing the next-nearest-neighbor hopping strength $|t'|$. Phase diagrams of V_0 versus U and $|t'|$ for various modulations of the spin order are presented. In addition, the quantum interference effect on the modulations of orders due to two strong nonmagnetic impurities is briefly examined, and the checkerboardlike and quasistripe patterns can occur depending on the sites where two impurities are placed.

DOI: 10.1103/PhysRevB.80.064518 PACS number(s): 74.20.−z, 74.25.Jb, 74.25.Ha

The impurity effect in high-temperature superconductors (HTSCs) has attracted considerable interest both experimentally and theoretically for many years as it may be a valuable probe into the mechanism of unconventional superconductivity.[1] Inelastic neutron scattering (INS) (Ref. 2) and angle-resolved photoemission spectroscopy (ARPES) (Ref. 3) measurements on the disparate effects of nonmagnetic Zn and magnetic Ni impurities can give insight into the pairing nature of HTSCs. High-resolution scanning-tunneling-microscopy (STM) experimental observations have been able to provide detailed local density of states (LDOS) images around single Zn (Ref. 4) and Ni (Ref. 5) impurities on the surface of $Bi_2Sr_2CaCu_2O_{8+x}$ (BSCCO). In particular, the nuclear magnetic resonance (NMR) measurements in $YBa_2Cu_3O_{7-x}$ (YBCO) have indicated that Zn/Li impurities enhance the antiferromagnetic (AFM) correlation and a staggered magnetic moment is induced on the Cu ions in the vicinity of the impurity sites.[6–8] Recent theoretical studies found that nonmagnetic scatterers can indeed generate the states of local magnetic moment tied to the impurity site.[9–12] The induction of the local magnetic state is related to the LDOS features probed by STM in cuprates. The formation of a spontaneous net spin $S_z=1/2$ moment is always associated with the substantial splitting of the LDOS resonance.[11] If the resonance observed around the impurity is without splitting,[4] it would be associated with the $S_z=0$ state. In the meanwhile, the quantum interference effect among multiple impurities has drawn much attention recently. The spatial distribution of the LDOS spectrum changes remarkably by varying the distance and orientation of the impurities.[13–15] The quantum interference between many impurities leads to definitive quasiparticle spectra in disordered *d*-wave superconductors,[16] and dopant disorder can stabilize novel states with antiferromagnetic order.[17]

On the other hand, intensive efforts have been focused on the inhomogeneous phase with stripe and checkerboard modulations in HTSCs for the past several years. Neutron scattering experimental observations of a peculiar static stripe phase in underdoped $La_{1.6-x}Nd_{0.4}Sr_xCuO_4$ supported that spatial modulations of spin and charge density are related to superconductivity.[18] NMR experiments on YBCO probed a strong AFM fluctuation around vortex cores, implying possible existence of spin density wave (SDW) order outside the vortex core.[19] A striking feature has revealed in the STM experiments by Hoffman *et al.*,[20] where a Cu-O bond-oriented four-unit-cell checkerboard pattern is localized in a small region near vortex cores in slightly overdoped BSCCO. Howald *et al.*[21] reported that the similar vortex-induced checkerboard modulations can survive even at zero magnetic field. Recently, the checkerboard pattern was also probed in the STM experiments for underdoped $Na_xCa_{2-x}CuO_2Cl_2$ (Ref. 22) and BSCCO (Ref. 23) samples. The one-dimensional (1D) stripe or two-dimensional (2D) structures of orders in cuprates have received substantial theoretical support.[24–34] A comparative study was made by Zhu *et al.*[25] for the spin and charge structures around superconducting vortices and impurities using an effective *t*-*U*-*V* Hubbard model and predicted that there is a SDW with a period of $8a$ around a unitary nonmagnetic impurity. It was also shown that the stripe modulation around nonmagnetic impurities could appear in the *d*-wave superconducting (DSC) and SDW orders.[11,35] However, so far, little attention has been paid to the transition of the modulations of orders around impurities as well as the quantum interference effect on that due to multiple impurities.

In the present work, we systematically investigate the impurity-induced modulations of orders in *d*-wave superconductors by numerically solving the Bogoliubov–de Gennes (BdG) equations based on a model Hamiltonian with competing AFM and DSC orders. Our numerical analysis concerns the transition of the modulations of orders around a single nonmagnetic impurity as a function of the strength of the AFM interaction and the impurity scattering strength as well as the hole doping. We also discuss the impurity-induced structures of SDW order in the case when the next-nearest-neighbor (nnn) hopping strength is varied. Finally, the quantum interference effect on the magnetization distribution due to two strong nonmagnetic impurities is exam-

ined. We expect our present results may provide useful information for future experiments.

We begin with an effective mean-field t-t'-U-V Hamiltonian by assuming that the on-site repulsion U is responsible for the competing AFM order and the nearest-neighbor attraction V for the DSC pairing,

$$H = -\sum_{\langle \mathbf{ij}\rangle,\sigma} t_{\mathbf{ij}} c^{\dagger}_{\mathbf{i}\sigma} c_{\mathbf{j}\sigma} + \sum_{\mathbf{i},\sigma} (U\langle n_{\mathbf{i}\bar{\sigma}}\rangle + V_0 \delta_{\mathbf{i},\mathbf{i}_m} - \mu) c^{\dagger}_{\mathbf{i}\sigma} c_{\mathbf{i}\sigma} + \sum_{\langle \mathbf{ij}\rangle} (\Delta_{\mathbf{ij}} c^{\dagger}_{\mathbf{i}\uparrow} c^{\dagger}_{\mathbf{j}\downarrow} + \Delta^{*}_{\mathbf{ij}} c_{\mathbf{j}\downarrow} c_{\mathbf{i}\uparrow}), \quad (1)$$

where $t_{\mathbf{ij}}=t$ and t' are the nearest-neighbor (nn) and nnn hopping integrals, respectively. $c_{\mathbf{i}\sigma}$ ($c^{\dagger}_{\mathbf{i}\sigma}$) are destruction (creation) operators for electron of spin σ, $n_{\mathbf{i}\sigma}=c^{\dagger}_{\mathbf{i}\sigma}c_{\mathbf{i}\sigma}$ is the number operator, and μ is the chemical potential determining the averaged electron density $\bar{n}=(1/N_xN_y)\Sigma_{\mathbf{i},\sigma}\langle n_{\mathbf{i}\sigma}\rangle$ ($N_x \times N_y$ is the linear dimension of the unit cell under consideration). $\mathbf{i}_m$ is the position of the impurity site, and V_0 is the single-site potential describing the scattering from nonmagnetic impurities. Our study is confined to the hole-doped system ($\bar{n}<1$), i.e., the hole doping $\delta=1-\bar{n}$. The SDW and DSC orders have the following definitions respectively: $\Delta^{SDW}_{\mathbf{i}}=U\langle c^{\dagger}_{\mathbf{i}\uparrow}c_{\mathbf{i}\uparrow}-c^{\dagger}_{\mathbf{i}\downarrow}c_{\mathbf{i}\downarrow}\rangle$ and $\Delta_{\mathbf{ij}}=V\langle c_{\mathbf{i}\uparrow}c_{\mathbf{j}\downarrow}-c_{\mathbf{i}\downarrow}c_{\mathbf{j}\uparrow}\rangle/2$. Using Bogoliubov transformation, $c_{\mathbf{i}\sigma}=\Sigma_n[u^n_{\mathbf{i}\sigma}\gamma_{n\sigma}-\sigma v^{n*}_{\mathbf{i}\sigma}\gamma^{\dagger}_{n\bar{\sigma}}]$, the mean-field Hamiltonian Eq. (1) can be diagonalized by solving the resulting BdG equations self-consistently,

$$\sum_{\mathbf{j}}^{N} \begin{pmatrix} \mathcal{H}_{\mathbf{ij}\sigma} & \Delta_{\mathbf{ij}} \\ \Delta^{*}_{\mathbf{ij}} & -\mathcal{H}^{*}_{\mathbf{ij}\bar{\sigma}} \end{pmatrix} \begin{pmatrix} u^n_{\mathbf{j}\sigma} \\ v^n_{\mathbf{j}\bar{\sigma}} \end{pmatrix} = E_n \begin{pmatrix} u^n_{\mathbf{i}\sigma} \\ v^n_{\mathbf{i}\bar{\sigma}} \end{pmatrix}, \quad (2)$$

where $\mathcal{H}_{\mathbf{ij}\sigma}=-t_{\mathbf{ij}}+[U\langle n_{\mathbf{i}\bar{\sigma}}\rangle+V_0\delta_{\mathbf{i},\mathbf{i_m}}-\mu]\delta_{\mathbf{ij}}$. With the periodic boundary conditions we can get the N positive eigenvalues (E_n) with eigenvectors ($u^n_{\mathbf{i}\uparrow}, v^n_{\mathbf{i}\downarrow}$) and negative eigenvalues ($\bar{E}_n$) with eigenvectors ($-v^{n*}_{\mathbf{i}\uparrow}, u^{n*}_{\mathbf{i}\downarrow}$). The self-consistent conditions are

$$\langle n_{\mathbf{i}\uparrow}\rangle = \sum_{n=1}^{2N} |\mathbf{u}^n_{\mathbf{i}}|^2 f(E_n), \quad (3)$$

$$\langle n_{\mathbf{i}\downarrow}\rangle = \sum_{n=1}^{2N} |\mathbf{v}^n_{\mathbf{i}}|^2 [1-f(E_n)], \quad (4)$$

$$\Delta_{\mathbf{ij}} = \sum_{n=1}^{2N} \frac{V}{4} (\mathbf{u}^n_{\mathbf{i}}\mathbf{v}^{n*}_{\mathbf{j}} + \mathbf{v}^{n*}_{\mathbf{i}}\mathbf{u}^n_{\mathbf{j}}) \tanh\left(\frac{E_n}{2k_BT}\right), \quad (5)$$

where $\mathbf{u}^n_{\mathbf{i}}=(-v^{n*}_{\mathbf{i}\uparrow}, u^n_{\mathbf{i}\uparrow})$ and $\mathbf{v}^n_{\mathbf{i}}=(u^{n*}_{\mathbf{i}\downarrow}, v^n_{\mathbf{i}\downarrow})$ are the row vectors, and $f(E)=(e^{E/k_BT}+1)^{-1}$ is the Fermi-Dirac distribution function. The DSC order parameter is defined at site i as $\Delta^D_{\mathbf{i}}=(\Delta_{\mathbf{i+e_x,i}}+\Delta_{\mathbf{i-e_x,i}}-\Delta_{\mathbf{i,i+e_y}}-\Delta_{\mathbf{i,i-e_y}})/4$, where $\mathbf{e_{x,y}}$ denotes the unit vector along the (x,y) direction. In our calculations, the distance is measured in units of the lattice constant a and the energy in the nn hopping integral parameter t. In the extreme limits of $U/V \gg 1$ or $U/V \ll 1$, the system is in either the SDW state or the pure d-wave superconducting state; whereas the coexistence of the SDW and superconducting orders may occur at intermediate values of U/V. For concentration, we set the pairing interactions $V=1.0$, the ratio of U to V varies in the range of (2.4–2.5). The nnn hopping t' has been chosen to fit the holelike Fermi surface of the cuprate superconductors. The averaged electron density is chosen as $\bar{n}=0.85$, corresponding to the optimally doped level $\delta=0.15$. The numerical calculation is performed on a unit cell of $N_x \times N_y = 32 \times 32$ sites. For an appropriate initial set of parameters $n_{\mathbf{i}\sigma}$ and $\Delta_{\mathbf{ij}}$, the Hamiltonian is numerically diagonalized and the electron wave functions obtained are used to calculate the new parameters for the next iteration step. The calculations was repeated until the difference in the order parameters between two consecutive iterations is less than 10^{-6}. A ground state has the lowest total energy among those of stable states evaluated from different possible initial parameters.

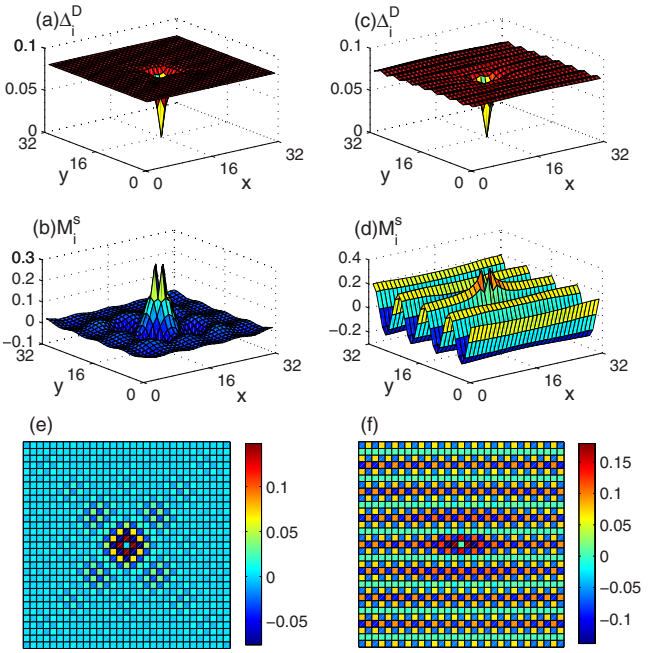

FIG. 1. (Color online) Spatial variations of the [(a) and (c)] DSC order parameter Δ^D_i and[(b) and (d)] staggered magnetization M^s_i as well as two-dimensional distribution of the [(e) and (f)] local moment S^z_i with a single nonmagnetic impurity at site (16,16) in a 32×32 lattice. The left and right panels are for the on-site repulsion $U_A=2.43$ and $U_B=2.44$, respectively. The averaged electron density is fixed at $\bar{n}=0.85$, and $t'=-0.25$, and $V_0=100$.

First let us choose $t'=-0.25$ and two U values: $U_A=2.43$ and $U_B=2.44$ such that both of the 1D stripe and 2D SDW modulations cannot be obtained in the absence of a magnetic field.[31] We introduce a nonmagnetic impurity such as Zn into our system at site (16,16) and investigate its effect. The on-site impurity potential is taken to be $V_0=100$. Figure 1 plots the spatial profiles of the DSC order parameter [(a) and (c)] and staggered magnetization [(b) and (d)] in a 32×32 lattice. Here, the staggered magnetization of the induced AFM or SDW order is defined as $M^s_i=(-1)^i(n_{i\uparrow}-n_{i\downarrow})$. The left panels in Fig. 1 are for $U_A=2.43$, where the 2D impurity-induced modulations of orders present. Note that, when magnetic field $B \neq 0$ and no impurities, the spin and charge orders display the field-induced stripe modulations.[31] From Fig. 1(a), one can easily see that the DSC order is dramatically suppressed at the impurity site and approaches

its bulk value at a few lattice constants away from the impurity. Due to the competition between the AFM order and the DSC order, the suppression of the DSC order may lead to the appearance of the AFM order. Moreover, a finite impurity potential acts as a local breaker of particle-hole symmetry that can modify the LDOS at the Fermi surface dramatically and induce a virtual bound state. In Fig. 1(b), it is clear that a 2D checkerboardlike SDW order is induced around the impurity and exhibits an oscillating behavior with a period of approximately 8a along both the x and y directions, which is similar to the vortex case in Ref. 25. The staggered moment of the SDW is zero at the impurity site and reaches the maximum value 0.3 at its four nn sites. The 2D spatial distribution of the impurity-induced local moment as defined by $S_i^z=(n_{i\uparrow}-n_{i\downarrow})/2$ is depicted in Fig. 1(e). It shows a staggered pattern localized around the impurity in agreement with NMR experiments.[7,8] A net spin $S_z=\Sigma_i S_i^z=1/2$ is generated, and the majority of the net moment resides on the four nearest neighbors of the impurity. Note that the NMR measurements in YBCO, which indicated spontaneous impurity-induced magnetization, are performed in the presence of a finite magnetic field generally. Harter *et al.*[12] investigated this case theoretically and obtained the similar impurity-induced staggered magnetization pattern. We also noticed that the static magnetism appears to exist even without an external field at low temperatures in $La_{1-x}Sr_xCuO_4$.[36,37] For an increased strength of the AFM interaction $U_B=2.44$, the 2D behavior of orders had been destroyed and the 1D stripe structures are present along the x axis [see the right panels in Fig. 1]. We notice that the striped DSC and SDW orders oscillate respectively with a period of $4a$ [Fig. 1(c)] and $8a$ [Fig. 1(d)], and the SDW order is pinned at the impurity site with one of its ridges. The obtained net moment still is $S_z=1/2$, while the spatial distribution of S_i^z displays a staggered stripe pattern in this case, as shown in Fig. 1(f).

To study the spatial modulation of the local moment phase, we present the phase diagram of impurity strength V_0 versus AFM interaction U in Fig. 2. It is obvious that the induced net moment $S_z=1/2$ should show up for larger V_0 and stronger U (the region above the red dashed line), while $S_z=0$ tends to exist for smaller V_0 or weaker U (the region below the red dashed line). In the region of local moment phase, there exist stripe and checkerboardlike modulations depending on the magnitude of the U value. As U is greater than U_c, the stripe modulation are intrinsic [stripe(i)].[31] The presence of a single impurity would slightly enhance the stripe modulation but does not modify the overall structure except the magnetizations at or very close to the impurity site are altered, as shown in Fig. 3(a). In the region of $U \leq U_c$, the impurity-induced SDW can show a stripe modulation which disappears with $B=0$ and no impurities [stripe(ii)]. If U goes far below U_c, the impurity-induced AFM order changes from the stripe to a 2D checkerboardlike SDW. Noticeably, the transition between stripe and checkerboardlike patterns can take place for different impurity strength. Figure 3(b) gives the spatial profiles of the staggered magnetization for a single impurity $V_0=5$ in contrast to Fig. 1(d). It is found that the induced SDW order no longer has the stripe structure but the net moment remains $S_z=1/2$. In addition, the phase diagram of V_0 versus hole doping δ

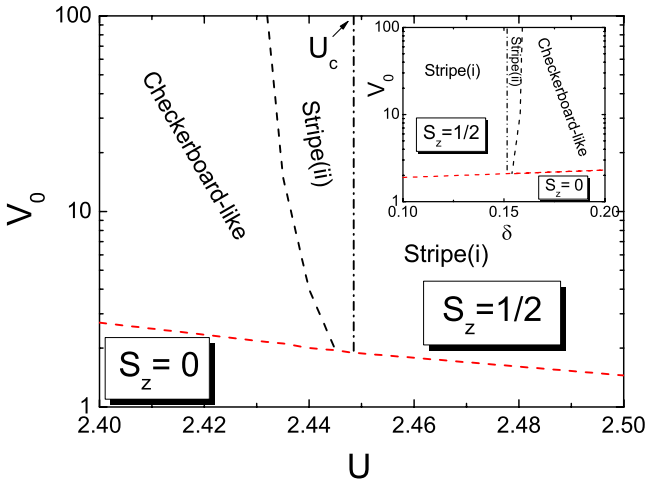

FIG. 2. (Color online) Phase diagram of V_0 versus interaction strength U with hole doping $\delta=0.15$ for different SDW order modulations around the impurity. Stripe(i) is the region where the stripe modulations are intrinsic and stripe(ii) corresponds to the region where the stripe modulations are impurity-induced. U_c denotes the critical on-site Coulomb interaction where the intrinsic stripe region [i.e., stripe(i)] occurs. Inset: phase diagram of V_0 versus hole doping δ with $U=2.45$.

with $U=2.45$ is plotted in the inset of Fig. 2. It is shown that the formation of the local moment (the region above the red dashed line) requires a larger impurity strength in the overdoped regime, and the stripe moment state can easily show up in the underdoped regime, because the induction of AFM order becomes more prominent at the lower doping case.

Next we turn to discuss the modulations of orders around a nonmagnetic impurity as the nnn hopping strength $|t'|$ is varied. The effect of nnn hopping t' is important, because the inclusion of t' in the Hubbard model is necessary to capture the electron-hole asymmetry.[38–40] Furthermore, t' is an important parameter in determining the charge orderings and their textures in cuprates.[33,34,41,42] We choose the same values of U and V_0 in Fig. 3(a) for our study, and the spatial variations of the staggered magnetization around a single impurity for different t' are plotted in Fig. 4. Figure 4(a) is for $t'=-0.27$, where the SDW order still shows stripe structure comparing with Fig. 3(a). The amplitude of the SDW stripe is weakly suppressed but its period not changed. Interest-

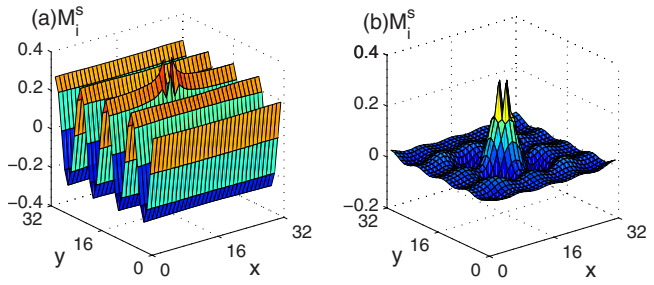

FIG. 3. (Color online) Spatial variations of the staggered magnetization M_i^s with a single nonmagnetic impurity at site (16,16) for (a) $U=2.5$, $V_0=100$ and (b) $U=2.44$, $V_0=5$. The other parameter values are: $\bar{n}=0.85$ and $t'=-0.25$.

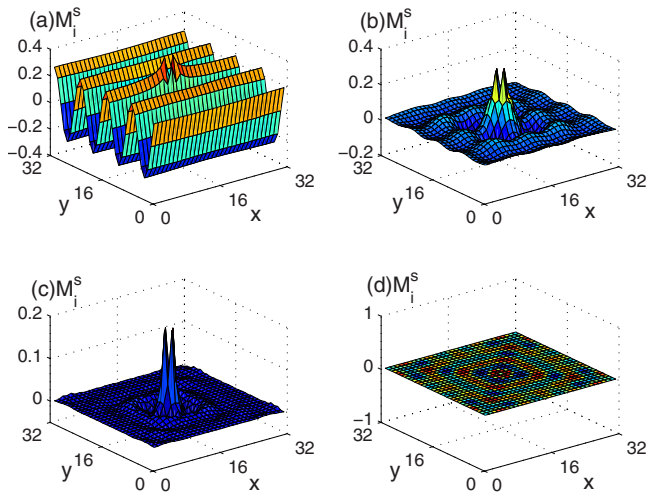

FIG. 4. (Color online) Spatial variations of the staggered magnetization M_i^s with a single nonmagnetic impurity at site (16,16) for (a) $t'=-0.27$, (b) $t'=-0.28$, (c) $t'=-0.40$, and (d) $t'=-0.45$. The other parameter values are: $\bar{n}=0.85$, $V_0=100$, and $U=2.5$.

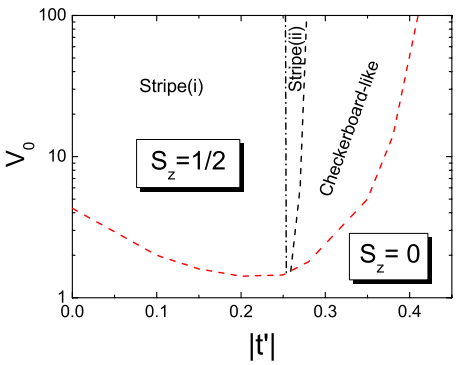

FIG. 5. (Color online) Phase diagram of V_0 versus nnn hopping strength $|t'|$ with $U=2.5$ and $\delta=0.15$ for different SDW order modulations around the impurity.

ingly, for a slight increased $|t'|$ (=0.28), the 1D stripe-ordered behavior is destroyed and a spatial distribution with 2D checkerboardlike modulation appears instead [see Fig. 4(b)]. At stronger nnn hopping strength (=0.40) the AFM order magnitude becomes smaller, and the impurity-induced staggered magnetization vanishes at a large distance from the impurity, indicating the appearance of the local AFM phase [see Fig. 4(c)]. Further increasing $|t'|$, the AFM order becomes extremely weak and the 2D SDW order is removed, as shown in Fig. 4(d). We notice that the net moment remains $S_z=1/2$ when the "*stripe*→*checkerboardlike*" transition takes place, while $S_z=0$ when the SDW order disappears in Fig. 4(d). In Fig. 5, the phase diagram of V_0 versus nnn hopping strength $|t'|$ is given. One can clearly see the transition of SDW order from 1D stripe to 2D checkerboardlike modulations in the "local moment phase" regime (above the red dashed line) with increasing $|t'|$. Interestingly, in contrast to the case for $t'=0$, the introduction of a small nnn hopping strength can enhance the AFM order. Corresponding to the staggered magnetization enhanced region, the impurity strength required to generate a local moment drops gradually and reaches a minimum at $t'\approx-0.2$. Further increasing $|t'|$, the staggered magnetization decreases and disappears near $t'=-0.41$, that is, a large nnn hopping would frustrate the antiferromagnetism. Consequently, the induced net moment should show up for larger impurity strength.

Finally, we would like to briefly examine the quantum interference effect on the SDW order due to two strong impurities. Another nn nonmagnetic impurity with $V_0=100$ is introduced into the stripe system with $S_z=1/2$ in Fig. 1(d), and the spatial distribution of the induced magnetization is shown in Fig. 6(a). It appears that, due to the cancellation effect of the two nn impurities, the maximum value of the induced staggered magnetization at the nn site of the impurities drops strongly and the AFM order is suppressed over the whole system in contrast to the single impurity case. Consequently, the 1D stripe transits to 2D checkerboardlike structure, and the net induced moment has $S_z=0$. For two strong impurities $V_0=100$ are placed at the nnn sites and at sites separated by a Cu ion, the induced spatial profiles of the staggered magnetization for $U=2.5$ and $t'=-0.28$ are, respectively, shown in Figs. 6(b) and 6(c). In both two cases, the induced AFM orders are enhanced in contrast to Fig. 5(b), and the net moment yields a local spin of $S_z=1$. Interestingly, in Fig. 6(c), a remarkable enhancement of the AFM order is shown at the central Cu site, and a quasistripe SDW modulation can occur due to the constructive interference effect. This kind of effect as well as the opposite destructive interference effect have been addressed in detail in Ref. 11.

In conclusion, we have investigated the impurity-induced structures of orders in *d*-wave superconductors by numerically solving the Bogoliubov–de Gennes equations based on a model Hamiltonian with competing AFM and DSC orders. We found that the transition between 1D stripe and 2D checkerboardlike modulations around a single nonmagnetic impurity can take place by tuning the strength of the AFM interaction or the impurity scattering strength. For different band structures, it was found that the impurity-induced stripe can first transit to checkerboardlike modulation and then

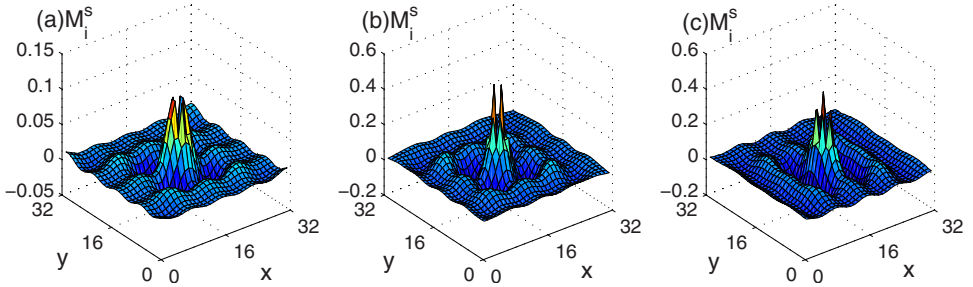

FIG. 6. (Color online) Spatial variations of the staggered magnetization M_i^s with (a) two nn impurities for $U=2.44$ and $t'=-0.25$, (b) two nnn impurities, and (c) two impurities separated by a Cu ion for $U=2.5$ and $t'=-0.28$. The other parameter values are: $\bar{n}=0.85$ and $V_0=100$.

disappears with increasing the nnn hopping strength. In addition, quantum interference effect between two nonmagnetic impurities can lead to checkerboardlike or quasistripe pattern depending on the sites where two impurities are placed. These phenomena are ready to be checked by the future experiments.

This work was supported by National Natural Science Foundation of China under Grant No. 60671042, by Shanghai leading academic discipline project under Grant No. S30105, by Shanghai Municipal Education Committee, by Flemish Science Foundation (FWO-V1), and by Belgian Science Policy (IAP).

*zgq_1981@shu.edu.cn

[1] A. V. Balatsky, I. Vekhter, and J.-X. Zhu, Rev. Mod. Phys. **78**, 373 (2006); H. Alloul, J. Bobroff, M. Gabay, and P. J. Hirschfeld, *ibid.* **81**, 45 (2009).
[2] Y. Sidis, P. Bourges, H. F. Fong, B. Keimer, L. P. Regnault, J. Bossy, A. Ivanov, B. Hennion, P. Gautier-Picard, G. Collin, D. L. Millius, and I. A. Aksay, Phys. Rev. Lett. **84**, 5900 (2000).
[3] K. Terashima, H. Matsui, D. Hashimoto, T. Sato, T. Takahashi, H. Ding, T. Yamamoto, and K. Kadowaki, Nat. Phys. **2**, 27 (2006).
[4] S. H. Pan, E. W. Hudson, K. M. Lang, H. Eisaki, S. Uchida, and J. C. Davis, Nature (London) **403**, 746 (2000).
[5] E. W. Hudson, K. M. Lang, V. Madhavan, S. H. Pan, H. Eisaki, S. Uchida, and J. C. Davis, Nature (London) **411**, 920 (2001).
[6] J. Bobroff, W. A. MacFarlane, H. Alloul, P. Mendels, N. Blanchard, G. Collin, and J.-F. Marucco, Phys. Rev. Lett. **83**, 4381 (1999).
[7] M.-H. Julien, T. Feher, M. Horvatic, C. Berthier, O. N. Bakharev, P. Segransan, G. Collin, and J.-F. Marucco, Phys. Rev. Lett. **84**, 3422 (2000)
[8] J. Bobroff, H. Alloul, W. A. MacFarlane, P. Mendels, N. Blanchard, G. Collin, and J.-F. Marucco, Phys. Rev. Lett. **86**, 4116 (2001).
[9] H. Tsuchiura, Y. Tanaka, M. Ogata, and S. Kashiwaya, Phys. Rev. B **64**, 140501(R) (2001).
[10] Z. Wang and P. A. Lee, Phys. Rev. Lett. **89**, 217002 (2002).
[11] Y. Chen and C. S. Ting, Phys. Rev. Lett. **92**, 077203 (2004).
[12] J. W. Harter, B. M. Andersen, J. Bobroff, M. Gabay, and P. J. Hirschfeld, Phys. Rev. B **75**, 054520 (2007).
[13] D. K. Morr and N. A. Stavropoulos, Phys. Rev. B **66**, 140508(R) (2002); **67**, 020502(R) (2003).
[14] L. Zhu, W. A. Atkinson, and P. J. Hirschfeld, Phys. Rev. B **67**, 094508 (2003).
[15] B. M. Andersen and P. Hedegard, Phys. Rev. B **67**, 172505 (2003).
[16] H. Y. Chen, L. Zhu, and C. S. Ting, Phys. Rev. B **73**, 172505 (2006).
[17] B. M. Andersen, P. J. Hirschfeld, A. P. Kampf, and M. Schmid, Phys. Rev. Lett. **99**, 147002 (2007).
[18] J. M. Tranquada, B. J. Sternlleb, J. D. Axe, Y. Nakamura, and S. Uchida, Nature (London) **375**, 561 (1995).
[19] V. F. Mitrovic, E. E. Sigmund, M. Eschrig, H. N. Bachman, W. P. Halperin, A. P. Reyes, P. Kuhns, and W. G. Moulton, Nature (London) **413**, 501 (2001).
[20] J. E. Hoffman, E. W. Hudson, K. M. Lang, V. Madhavan, S. H. Pan, H. Eisaki, S. Uchida, and J. C. Davis, Science (London) **295**, 466 (2002).
[21] C. Howald, H. Eisaki, N. Kaneko, and A. Kapitulnik, arXiv:cond-mat/0201546 (unpublished).
[22] T. Hanaguri, C. Lupien, Y. Kohsaka, D. H. Lee, M. Azuma, M. Takano, H. Takagi, and J. C. Davis, Nature (London) **430**, 1001 (2004).
[23] K. McElroy, D. H. Lee, J. E. Hoffman, K. M. Lang, J. Lee, E. W. Hudson, H. Eisaki, S. Uchida, and J. C. Davis, Phys. Rev. Lett. **94**, 197005 (2005).
[24] V. J. Emery, S. A. Kivelson, and J. M. Tranquada, Proc. Natl. Acad. Sci. U.S.A. **96**, 8814 (1999).
[25] J.-X. Zhu, I. Martin, and A. R. Bishop, Phys. Rev. Lett. **89**, 067003 (2002).
[26] H. D. Chen, J. P. Hu, S. Capponi, E. Arrigoni, and S. C. Zhang, Phys. Rev. Lett. **89**, 137004 (2002).
[27] A. Polkovnikov, M. Vojta, and S. Sachdev, Phys. Rev. B **65**, 220509(R) (2002).
[28] Y. Chen, H. Y. Chen, and C. S. Ting, Phys. Rev. B **66**, 104501 (2002).
[29] D. Podolsky, E. Demler, K. Damle, and B. I. Halperin, Phys. Rev. B **67**, 094514 (2003).
[30] B. M. Andersen, P. Hedegard, and H. Bruus, Phys. Rev. B **67**, 134528 (2003).
[31] H. Y. Chen and C. S. Ting, Phys. Rev. B **71**, 220510(R) (2005).
[32] J. A. Robertson, S. A. Kivelson, E. Fradkin, A. C. Fang, and A. Kapitulnik, Phys. Rev. B **74**, 134507 (2006).
[33] G. Seibold, J. Lorenzana, and M. Grilli, Phys. Rev. B **75** 100505(R) (2007).
[34] G. Q. Zha, H. W. Zhao, and S. P. Zhou, Phys. Rev. B **76**, 132503 (2007).
[35] H. Y. Chen and C. S. Ting, Phys. Rev. B **68**, 212502 (2003).
[36] B. Lake, H. M. Ronnow, N. B. Christensen, G. Aeppli, K. Lefmann, D. F. McMorrow, P. Vorderwisch, P. Smeibidl, N. Mangkorntong, T. Sasagawa, M. Nohara, H. Takagi, and T. E. Mason, Nature (London) **415**, 299 (2002).
[37] H. Kimura, M. Kofu, Y. Matsumoto, and K. Hirota, Phys. Rev. Lett. **91**, 067002 (2003).
[38] R. J. Gooding, K. J. E. Vos, and P. W. Leung, Phys. Rev. B **50**, 12866 (1994).
[39] T. Tohyama and S. Maekawa, Phys. Rev. B **49**, 3596 (1994); Supercond. Sci. Technol. **13**, R17 (2000).
[40] A. Macridin, M. Jarrell, Th. Maier, and G. A. Sawatzky, Phys. Rev. B **71**, 134527 (2005).
[41] S. R. White and D. J. Scalapino, Phys. Rev. B **60**, R753 (1999).
[42] A. Himeda, T. Kato, and M. Ogata, Phys. Rev. Lett. **88**, 117001 (2002).